Hindawi
Mathematical Problems in Engineering
Volume 2022, Article ID 5163609, 14 pages
https://doi.org/10.1155/2022/5163609

Research Article

Stability Analysis of COVID-19 Epidemic Model of Type *SEIQHR* with Fractional Order

Sid Ahmed Ould Beinane,[1] **Mohamed Reda Lemnaouar**,[2] **Rabie Zine**,[3] **and Younes Louartassi**[2]

[1]*RT-M2A Laboratory, Mathematics Department, College of Science Jouf University, P.O. Box: 2014, Sakaka, Saudi Arabia*
[2]*Mohammed V University in Rabat, High School of Technology of Salé, LASTIMI, Salé, Morocco*
[3]*School of Science and Engineering, Al Akhawayn University in Ifrane, Ifrane, Morocco*

Correspondence should be addressed to Rabie Zine; r.zine@aui.ma

Received 11 May 2022; Revised 2 August 2022; Accepted 3 September 2022; Published 26 September 2022

Academic Editor: Akif Akgul

In this article, we consider a fractional *SEIR* model, denoted by the *SEIQHR* model, which aims to predict the outbreak of infectious diseases in general. In particular, we study the spread of COVID-19. The fractional order offers a flexible, appropriate, and reliable framework for pandemic growth characterization. Firstly, we analyze some elementary results of the model (boundedness and uniqueness of solutions). In addition, we establish certain conditions to ensure the local stability of the disease-free and endemic equilibrium points. Based on analytical and numerical results, we conclude that coronavirus infection (COVID-19) remains endemic, which requires long-term prevention and intervention strategies.

1. Introduction

COVID-19 represents the disease caused by a virus in the *Coronaviridae* family, and SARS-CoV-2 appeared at the end of 2019 in Wuhan, China [1]. It spread rapidly around the world, causing a worldwide epidemic [2, 3].

COVID-19 is a respiratory illness that can be fatal for old patients or other chronic diseases. It is transmitted through close contact with infected people. The disease could also be spread by asymptomatic patients [4], but scientific data are lacking to attest with certainty. In addition, the international health organization has imposed security measures to control the spread including isolation, quarantine, increased home confinement, promotion of wearing face masks, travel restrictions, the closure of public space, and the cancellation of events. The number of confirmed cases increased rapidly to reach more than 517 million cases, and approximately 6.25 million deaths were recorded worldwide as of May 2022.

There are several *SEIR* (susceptible-exposed-infectious-recovered) models that study infectious diseases in general [5–7]; since the appearance of the virus, the *SEIR* models proposed aim to study the behavior of this epidemic [8].

In the last decade, fractional models have been used to model diseases in general. For example, Singh [9] proposed a new fractional model of blood alcohol model using the Hilfer fractional operator. Kumar et al. [10] proposed a model to study the transmission dynamics of dengue, and they considered the generalized Caputo fractional operator. Since the apparition of COVID-19, researchers have used fractional derivatives used in the modeling of this infectious disease. As an example, the work in [11–15] has developed the classic *SEIR* model known by fractional models (*SEIQHR* and *SEIQR d*) for epidemic analysis of COVID-19 worldwide. This development is founded on the establishment of new quarantine conditions and the hospitalization of confirmed cases, which are considered as epidemic parameters for COVID-19. Recently, many types of fractional derivatives have been employed to model the propagation of COVID-19. For instance, Danane et al. proposed a fractional-order model of the disease (COVID-19) with government action and individual response by the Caputo

operator. Bonyah et al. used the Atangana–Baleanu operator for investigating the fractional optimal control dynamics of a coronavirus model. Yadav et al. studied the dynamics of the fractional-order COVID-19 model with memory effect using the Liouville–Caputo operator, so they employed the Adams–Bashforth–Moulton approach to find an approximate solution. Consequently, this development shows us more precisely the behavior of this epidemic.

Recently, fractional calculus has shown wide applicability in many fields, which can be obtained by extracting a dynamic behavior of biological systems shown by a mathematical formulation of integer derivatives. Fractional models have been proposed to study several phenomena involving the memory effect, including epidemic behavior [16], and they offer more flexibility than classical integer-order models to fit the data accurately [17]. Several researchers presented the differential fractional theory [18–21] for this reason, and many papers studied fractional biological models [22, 23]. Recently, new types of fractional derivatives have been developed. For instance, Khalil et al. [24] proposed a new fractional derivative and its properties. Subsequently, Abdeljawad [25] developed the properties of the conformable fractional derivative. After that, Benmakhlouf et al. [26] studied the finite time stability (FTS) and finite time boundedness (FTB) of the conformable fractional derivative. Currently, Hattaf [27, 28] introduced a new definition of the fractional derivative with a non-singular kernel in the sense of Caputo to generalize the various types by making these properties, and he proposed an approach for studying the stability of the latter. After that, Hattaf et al. [29] proposed a new numerical method for approximating the generalized Hattaf fractional derivative involving a non-singular kernel based on Lagrange polynomial interpolation.

Inspired by the aforementioned work and previous literature, we provide the compartmental model of COVID-19 with a standard incidence rate explored in [30] considering fractional Caputo derivatives for a better insight into the disease. The aim of the epidemic model (4) is to describe the dynamic behavior of the disease and predict the tendency for the disease to spread. Therefore, we have proposed a *SEIQHR* model. First, we analyze the qualitative properties of this model, including the existence and uniqueness of the disease-free and endemic equilibrium points. Second, we establish the conditions to ensure local asymptotic stability of disease-free and endemic equilibrium points. Third, we study the contribution of parameters to reproductive numbers. At the end, a numerical simulation is proposed to show the behavior of the different compartments of our model (4), and we will give some clarification into the interpretation and role of fractional derivatives.

2. Preliminary Results

We begin by giving some definitions of fractional calculus.

Definition 1 (see [31]). The Caputo fractional derivate of function f order is defined by

$$\begin{aligned} d^{\beta} f(t) &= d^{-(n-\beta)} \frac{d^n}{dt^n} (f(t)) \\ &= \frac{1}{\Gamma(n-\beta)} \int_0^t f^{(n)}(x)(t-x)^{n-\beta-1} dx, \end{aligned} \tag{1}$$

where $n-1 \le \beta < n \in \mathbb{N}^*$.

Definition 2 (see [32]). *Let the fractional system*

$$\begin{cases} d^{\beta} X(t) = f(t, X), t > 0, \\ X(t_0) = X_0 > 0, \end{cases} \tag{2}$$

where $\beta \in [0,1], t_0 > 0$, *and* $f: [t_0, +\infty[\times \Omega \longrightarrow \mathbb{R}^n, \Omega \subset \mathbb{R}^n$. *If* $f(t, X)$ *fulfill the local Lipschitz condition with respect to* X, *there exists a unique solution of the above system.*

Lemma 1 (see [33]). *Let the fractional-order system*

$$\begin{cases} d^{\beta} x(t) = f(x), t > 0, \\ x(t_0) = x_0 > 0, \end{cases} \tag{3}$$

with $0 \le \beta < 1, x \in \mathbb{R}$. *The equilibrium points of the above system are calculated by solving the following equation:* $f(x) = 0$. x^* *are locally asymptotically stable if all eigenvalues* λ *of the Jacobian matrix* $J = \partial f / \partial x$ *at* x^* *evaluated of the equilibrium points satisfy Matignon's condition (see [34])* $|arg(\lambda)| > \beta\pi/2$.

3. Description of Model

In this section, we present a mathematical formulation to model the behavior of compartments; first we will split our population into six categories $S(t)$ Susceptible, $E(t)$ Exposed, $I(t)$ Infected, $Q(t)$ Quarantined, $H(t)$ Hospitalized and $R(t)$Recovered. The description of the parameters is indicated in Table 1, so that the description of the interactions between the compartments is illustrated in Figure 1. The incidence rate plays an important role in describing the evolution of an infectious disease. Based on the spread of different diseases, there are many forms of incidence rates [30, 35–37]. In our model, we assume the bilinear incidence rates [30] ($\beta_1 SI$ and $\beta_2 SE$). Thus, our proposed model (4) is in the following form:

$$\begin{cases} d^{\beta} S(t) = \Lambda - \beta_1 SI - \beta_2 SE - dS - a_s S, \\ d^{\beta} E(t) = \beta_1 SI + \beta_2 SE - \alpha E - dE, \\ d^{\beta} I(t) = \alpha E - \delta I - \eta I - \mu I - dI, \\ d^{\beta} Q(t) = \delta I - kQ - \varepsilon Q - dQ, \\ d^{\beta} H(t) = \varepsilon Q + \eta I - rH - dH, \\ d^{\beta} R(t) = rH + \mu I - dR - a_r R, \end{cases} \tag{4}$$

with initial conditions

$$S(0) \ge 0,\ E(0) \ge 0,\ I(0) \ge 0,\ Q(0) \ge 0,\ H(0) \ge 0 \text{ and } R(0) \ge 0, \tag{5}$$

where d^{β} is in the sense of Caputo fractional derivative and $0 < \beta \le 1$.

Table 1: Description of variables and parameters.

VARS and PRM	Explanation
S	Susceptible individuals
E	Exposed individuals
I	Infected individuals
Q	Quarantined individuals
H	Hospitalized individuals
R	Recovered individuals
Λ	Inflow number of susceptible individuals
β_1	Infection rates of the infected individuals
β_2	Infection rates of the exposed individuals
α	Incubation rate
δ	Rate at which symptomatic infections are diagnosed and quarantined
d	Natural rate mortality
μ	Rate at which symptomatic infections are diagnosed and recovered
η	Rate at which symptomatic infections are diagnosed and hospitalized
ε	Transition rate of quarantined individuals to the hospitalized infected class
r	Transition rate of hospitalized individuals to the recovered class
k	The death rate caused by the disease

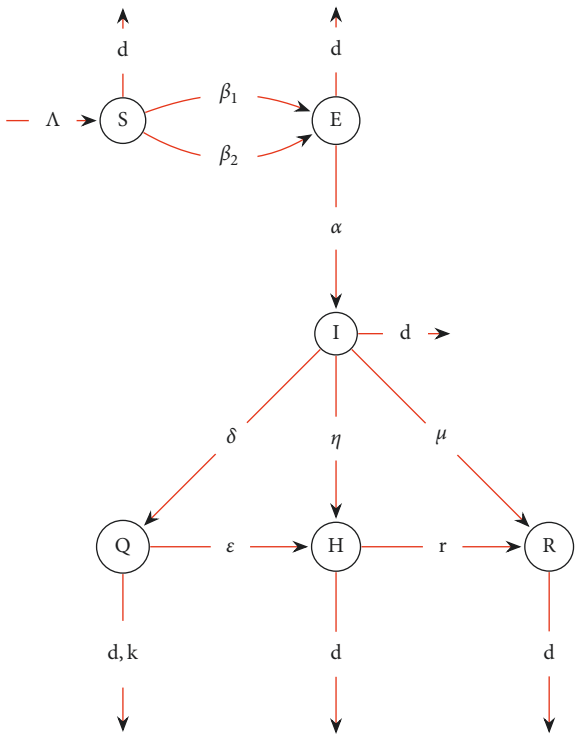

Figure 1: Schematic diagram of (4).

Our model (4) is based on the following hypothesis. (H_1): the number of susceptible individuals added is constant each day. (H_2): the susceptible individuals (S) move into the exposed (E) class before the infected class. (H_3): when an individual is infected (I), he is either quarantined (Q), hospitalized (H) (severe case), or recovered. (H_4): a confined individual can be hospitalized if his situation is critical.

The detailed description of (4) is presented in the following schema.

4. Boundedness and Uniqueness of Solutions

This section is dedicated to demonstrate the boundedness of the solutions of (4).

Lemma 2. *The set* $\Omega = \{(S, E, I, Q, H, R) \in \mathbb{R}_+^6 : N(t) \leq N(0) + \Lambda/d\}$ *is a region of attraction for all solutions initiating in the interior of the positive octant, where* $N = S + E + I + Q + H + R$.

Proof 1. We pose $N(t) = S(t) + E(t) + I(t) + Q(t) + H(t) + R(t)$; then,

$$d^\beta N + dN = \Lambda - kQ \leq \Lambda. \tag{6}$$

Using the theory of fractional inequality (see [31]), we obtain

$$N(t) \leq N(0) E_\beta\left(-dt^\beta\right) + \frac{\Lambda}{d}\left(1 - E_\beta\left(-dt^\beta\right)\right), \tag{7}$$

where $E_\beta(z) = \sum_{k=0}^{\infty} z^k/\Gamma(\beta k + 1)$ is Mittag-Leffler function [31], $\Gamma(z) = \int_0^\infty x^{z-1}e^{-x}dx$ is Euler's gamma function, and $0 < E_\beta(-dt^\beta) \leq 1$ if $t \longrightarrow \infty$, and we have $0 < N(t) \leq N(0) + \Lambda/d$, proving this lemma.

Otherwise, model (4) is equivalent to the model:

$$d^\beta X = F(X), \tag{8}$$

where

$$X = \begin{pmatrix} S \\ E \\ I \\ Q \\ H \\ R \end{pmatrix},$$

$$F(X) = \begin{pmatrix} \Lambda - \beta_1 SI - \beta_2 SE - dS \\ \beta_1 SI + \beta_2 SE - \alpha E - dE \\ \alpha E - \delta I - \eta I - \mu I - dI \\ \delta I - kQ - \varepsilon Q - dQ \\ \varepsilon Q + \eta I - rH - dH \\ rH + \mu I - dR \end{pmatrix} = \begin{pmatrix} F_1(X) \\ F_2(X) \\ F_3(X) \\ F_4(X) \\ F_5(X) \\ F_6(X) \end{pmatrix}. \tag{9}$$

□

Theorem 1. *Assume that the initial conditions $X(0) \geq 0$. Then, there exists a unique solution of system (4) defined on$0, +\infty$.*

The sufficient condition for the existence and uniqueness of the solution of system (4) in the region $\Omega \times [t_0, T]$with initial conditions $X(0)$ and $L = \max(d + 2(\beta_1 + \beta_2)M, d + 2(\alpha + \beta_2 M), d + 2(\eta + \mu + \delta + \beta_1 M), d + k + 2\varepsilon, (d + 2r), d$ is $\|F(X)-F(X')\| 1 \leq L\|X-X'\| 1$..

Proof 2. To prove the global existence and uniqueness of (4), consider the region $\Omega \times [t_0, T]$, where $\Omega = \{(S, E, I, Q, H, R) \in \mathbb{R}^{+6}: \max\{|S|, |E|, |I|, |Q|, |H|, |R|\} \leq M, M > 0\}$.

For any $X = (S, E, I, Q, H, R)^T$, $X' = (S', E', I', Q', H', R')^T \in \Omega$,

$$\begin{aligned}
\left\|F(X) - F(X')\right\|_1 &= \sum_{i=1}^{6} \left|F_i(X) - F_i(X')\right| \\
&= \left|\beta_1(SI - S'I') + \beta_2(\mathrm{SE} - S'E') + d(S - S')\right| + \left|\beta_1(SI - S'I') + \beta_2(\mathrm{SE} - S'E') - (\alpha + d)(E - E')\right| \\
&\quad + \left|\alpha(E - E') - (\delta + \eta + \mu + d)(I - I')\right| + \left|\delta(I - I') - (k + d + \varepsilon)(Q - Q')\right| \\
&\quad + \left|\varepsilon(Q - Q') + \eta(I - I') - (r + d)(H - H')\right| + \left|r(H - H') + \mu(I - I') - d(R - R')\right| \\
&\leq (d + 2(\beta_1 + \beta_2)M)\left|S - S'\right| + (d + 2(\alpha + \beta_2 M))\left|E - E'\right| + (d + 2(\eta + \mu + \delta + \beta_1 M))\left|I - I'\right| \\
&\quad + (d + k + 2\varepsilon)\left|Q - Q'\right| + (d + 2r)\left|H - H'\right| + d\left|R - R'\right| \leq L\left\|X - X'\right\|_1,
\end{aligned} \tag{10}$$

where

$$L = \max(d + 2(\beta_1 + \beta_2)M, d + 2(\alpha + \beta_2 M), d + 2(\eta + \mu + \delta + \beta_1 M), d + k + 2\varepsilon, (d + 2r), d). \tag{11}$$

Thus, F satisfies Lipschitz's condition (see [32] and Definition 2) with respect to X. □

5. Equilibria and Local Stability

In the first part of this section, we debate the existence of equilibria. It is evident that (4) has an infection-free equilibrium $P_0(\Lambda/d, 0, 0, 0, 0, 0)$. Also, other endemic equilibrium point $P^*(S^*, E^*, I^*, Q^*, H^*, R^*)$ is defined after in (13). The basic reproduction number of (4) is

$$R_0 = \frac{\Lambda(\beta_1\alpha + \beta_2(\delta + \mu + d + \eta))}{(d + a_s)(\delta + \mu + d + \eta)(\alpha + d)}. \tag{12}$$

Theorem 2.

(1) If $R_0 \leq 1$, then system (4) has one infection-free equilibrium$P_0(\Lambda/d, 0, 0, 0, 0, 0)$.

(2) If $R_0 > 1$, then (4) has endemic equilibrium point$P^*(S^*, E^*, I^*, Q^*, H^*, R^*)$, where$(S^*, E^*, I^*, Q^*, H^*, R^*)$are defined after in (9).

Proof 3. To get the endemic equilibrium point of the (4), in the interior of the equilibrium $P^*(S^*, E^*, I^*, Q^*, H^*, R^*)$, □

Proof. i.e., $F_i(S, E, I, Q, H, R) = 0$ for $i = 1, \ldots, 6$, we get

$$\begin{aligned}
S^* &= \frac{\Lambda(\delta + \mu + d + \eta)}{\beta_1\alpha E^* + (\beta_2 E^* + d)(\delta + \mu + d + \eta)}, \\
I^* &= \frac{\alpha E^*}{\delta + \mu + d + \eta}, \\
Q^* &= \frac{\delta\alpha E^*}{(k + d + \varepsilon)(\delta + \mu + d + \eta)}, \\
H^* &= \frac{[\eta(\varepsilon + k + d) + \varepsilon\delta]\alpha E^*}{(k + d + \varepsilon)(r + d)(\delta + \mu + d + \eta)}, \\
R^* &= \frac{(r[\eta(\varepsilon + k + d) + \varepsilon\delta] + \mu(r + d)(k + d + \varepsilon))\alpha E^*}{(k + d + \varepsilon)(r + d)(\delta + \mu + d + \eta)d}, \\
E^* &= \frac{(\delta + \mu + d + \eta)d}{\beta_1\alpha + \beta_2(\delta + \mu + d + \eta)}(R_0 - 1).
\end{aligned} \tag{13}$$

Then, if $R_0 > 1$, then (4) has endemic equilibrium point P^*.

Now, we analyzed the local asymptotic stability of disease-free equilibrium point P_0 and endemic equilibrium point P^* for (4). □

Theorem 3. *The disease-free equilibrium point P_0 is locally asymptotically stable, if $\delta + \mu + \eta + 2\ d + \alpha > \beta_2\Lambda/d$ and $R_0 < 1$.*

Proof 5. To prove the local stability of equilibria, the eigenvalues of the Jacobian matrix of (4) are evaluated by

$$J_0 = \begin{pmatrix} J_{11} & J_{12} \\ J_{21} & J_{22} \end{pmatrix}, \tag{14}$$

where

$$J_{11} = \begin{pmatrix} -d & 0 & 0 \\ \frac{-\beta_2\Lambda}{d} & \frac{\beta_2\Lambda}{d} - (\alpha + d) & \alpha \\ \frac{-\beta_1\Lambda}{d} & \frac{\beta_1\Lambda}{d} & -(\delta + \mu + d + \eta) \end{pmatrix},$$

$$J_{12} = \begin{pmatrix} 0 & 0 & 0 \\ 0 & 0 & 0 \\ \delta & \eta & \mu \end{pmatrix},$$

$$J_{21} = \begin{pmatrix} 0 & 0 & 0 \\ 0 & 0 & 0 \\ 0 & 0 & 0 \end{pmatrix},$$

$$J_{22} = \begin{pmatrix} -(d + \varepsilon + k) & \varepsilon & 0 \\ 0 & -(r + d) & r \\ 0 & 0 & -d \end{pmatrix}. \tag{15}$$

The characteristic equation of $P_0(\Lambda/d, 0, 0, 0, 0, 0)$ is

$$(\lambda + d)^2 (\lambda + r + d)(\lambda + k + d + \varepsilon)\left(\lambda^2 + s\lambda + p\right) = 0, \tag{16}$$

where $s = \delta + \mu + \eta + 2\ d + \alpha - \beta_2\Lambda/d$, $p = (\delta + \mu + \eta + d)(d + \alpha - \beta_2\Lambda/d) - \alpha\beta_1\Lambda/d = (d + \alpha)(\delta + \mu + \eta + d)(1 - R_0)$.

The discriminant of equation $\lambda^2 + s\lambda + p = 0$ is $(\delta + \mu + \eta - \alpha + \beta_2\Lambda/d)^2 + 4\Lambda\alpha\beta_1/d > 0$. Then, the eigenvalues of matrix (10) to the equilibrium point P_0 are reel roots, so $\lambda_1 = -(k + d + \varepsilon) < 0$, $\lambda_2 = -(r + d) < 0$, $\lambda_3 = \lambda_4 = -d < 0$, $\lambda_5 + \lambda_6 = -s$, and $\lambda_5\lambda_6 = p$.

If $s > 0$ and $R_0 < 1$, then $\lambda_5 + \lambda_6 < 0$ and $\lambda_5\lambda_6 > 0$. So, $\lambda_5 < 0$ and $\lambda_6 < 0$. The proof is completed. □

Theorem 4. *The endemic equilibrium point P^* is locally asymptotically stable if $R_0 > 1$ and condition (12) are realized.*

Proof 6. In the same way as the previous proof, let

$$J^* = \begin{pmatrix} J_{11}^* & J_{12}^* \\ J_{21}^* & J_{22}^* \end{pmatrix}, \tag{17}$$

where

$$J_{11}^* = \begin{pmatrix} -(\beta_1 I^* + \beta_2 E^* + d) & \beta_1 I^* + \beta_2 E^* & 0 \\ -\beta_2 S^* & \beta_2 S^* - (\alpha + d) & \alpha \\ -\beta_1 S^* & \beta_1 S^* & -(\delta + \mu + d + \eta) \end{pmatrix},$$

$$J_{12}^* = \begin{pmatrix} 0 & 0 & 0 \\ 0 & 0 & 0 \\ \delta & \eta & \mu \end{pmatrix},$$

$$J_{21}^* = \begin{pmatrix} 0 & 0 & 0 \\ 0 & 0 & 0 \\ 0 & 0 & 0 \end{pmatrix},$$

$$J_{22}^* = \begin{pmatrix} -(d + \varepsilon + k) & \varepsilon & 0 \\ 0 & -(r + d) & r \\ 0 & 0 & -d \end{pmatrix}. \tag{18}$$

From the Jacobian matrix J^*, the characteristic equation at P^* is

$$(\lambda + d)(\lambda + r + d)(\lambda + k + d + \varepsilon)\left(\lambda^3 + a_2\lambda^2 + a_1\lambda + a_0\right) = 0, \tag{19}$$

where

$$\begin{aligned} a_0 &= (\delta + \mu + \eta + d)\left((\beta_1 I^* + \beta_2 E^* + d)(\alpha + d) - d\beta_2 S^*\right) \\ &\quad - \alpha\ d\beta_1 S^*, \\ a_1 &= (\delta + \mu + \eta + d)\left(\alpha + 2\ d + \beta_1 I^* + \beta_2 E^* - \beta_2 S^*\right) \\ &\quad + (\beta_1 I^* + \beta_2 E^* + d)(\alpha + d) - (\beta_1\alpha + d\beta_2)S^*, \\ a_2 &= \beta_1 I^* + \beta_2 E^* + 3\ d + \alpha - \beta_2 S^* + \delta + \mu + \eta. \end{aligned} \tag{20}$$

Using (13), we get

$$a_0 = dS^* \left(\alpha\beta_1 + \beta_2 (\eta + \mu + d + \delta)\right)(R_0 - 1) > 0,$$

because $R_0 > 1$,

$$a_1 = (\delta + \mu + \eta + \alpha + 2\ d)dR_0 - \frac{\beta_2 \Lambda}{R_0}, \tag{21}$$

$$a_2 = \delta + \mu + \eta + \alpha + 2\ d + dR_0 - \frac{\beta_2 \Lambda}{dR_0}.$$

Firstly, $\lambda_1 = -d < 0$, $\lambda_2 = -(r + d) < 0$, $\lambda_3 = -(k + d + \varepsilon) < 0$. Then, $|\arg(\lambda_{1,2,3})| = \pi > \beta\pi/2$.

On the other hand, the discriminant of algebraic equation $\lambda^3 + a_2\lambda^2 + a_1\lambda + a_0 = 0$ is this form (see [38]):

$$d(P) = 18a_1a_2a_0 + (a_2a_1)^2 - 4a_1^3 - 4a_2^3a_0 - 27a_0^2. \tag{22}$$

Then, the equilibrium point P^* is locally asymptotically stable in one of the following cases:

(1) If $d(P) > 0$, P^* is asymptotically stable if $a_1, \quad a_2 > 0$ and $a_2a_1 - a_0 > 0 \quad$ for all $\beta \in 0, 1$.

(2) If $d(P) < 0$ and $a_1, a_2 > 0$, P^* is asymptotically stable if $\beta < 2/3$ and $a_2a_1 - a_0 > 0$.

(3) If $d(P) < 0$, $a_1, a_2 > 0$ and $a_2a_1 = a_0$, P^* is asymptotically stable for all $\beta \in 0, 1$.

Then, P^* is locally asymptotically stable if $R_0 > 1$ and (12) are realized. □

6. Sensitivity Analysis

Sensitivity analysis shows us the impact of each parameter on the transmission of the disease. It is used to understand which parameters have a high impact on the R_0 threshold. More specifically, sensitivity indices allow us to measure the relative change in a variable when a parameter changes. If this variable is differentiable with respect to the parameter, the sensitivity index is defined as follows [39]:

$$S_a^{R_0} = \frac{\partial R_0}{\partial a}\frac{a}{R_0}, \tag{23}$$

where a represent the contribution to the basic reproductive number R_0.

For Λ, $S_\Lambda^{R_0} = \partial R_0/\partial\Lambda\,(\Lambda/R_0) = 1$.

For β_1, $S_{\beta_1}^{R_0} = \partial R_0/\partial\beta_1\,(\beta_1/R_0) = \alpha\beta_1/\alpha\beta_1 + \beta_2(\delta + \mu + \eta + d)$.

For β_2, $S_{\beta_2}^{R_0} = \partial R_0/\partial\beta_2\,(\beta_2/R_0) = \beta_2(\delta + \mu + \eta + d)/\alpha\beta_1 + \beta_2(\delta + \mu + \eta + d)$.

For μ, $S_\mu^{R_0} = \partial R_0/\partial\mu\,(\mu/R_0) = -(\beta_1\alpha\mu/(\alpha\beta_1 + \beta_2(\delta + \mu + \eta + d))(\delta + \mu + \eta + d))$.

For η, $S_\eta^{R_0} = \partial R_0/\partial\eta\,(\eta/R_0) = -(\beta_1\alpha\eta/(\alpha\beta_1 + \beta_2(\delta + \mu + \eta + d))(\delta + \mu + \eta + d))$.

For δ, $S_\delta^{R_0} = \partial R_0/\partial\delta\,(\delta/R_0) = -(\beta_1\alpha\delta/(\alpha\beta_1 + \beta_2(\delta + \mu + \eta + d))(\delta + \mu + \eta + d))$.

For α, $S_\alpha^{R_0} = \partial R_0/\partial\alpha \cdot (\alpha/R_0) = (\alpha(\beta_1 d - \beta_2(\delta + \mu + \eta + d))/(\alpha + d)(\alpha\beta_1 + \beta_2(\delta + \mu + \eta + d)))$.

Table 2: Sensitivity index of the basic reproduction number.

Parameters	Sensitivity index
Λ	+1
β_1	+0.1523
β_2	+0.8477
μ	−0.063
η	−0.0253
δ	−0.064
α	−0.2252
d	−0.9401

For d, $S_d^{R_0} = \partial R_0/\partial d \cdot (d/R_0) = -(\beta_1((d + \alpha)(d + \eta + \mu + \delta) + d(d + \alpha) + d(d + \eta + \mu + \delta)/(d + \alpha)(d + \eta + \delta + \mu)(\beta_1\alpha + \beta_1(\mu + \delta + \eta + d))) + (\beta_2(2\ d + \alpha)(d + \mu + \eta + \delta)/(d + \alpha)(\beta_1\alpha + \beta_1(\mu + \delta + \eta + d))))$. Using the values of parameters (14), we get the following table.

The sensitivity index can depend on the system parameters, but it can also be constant. For example, $S_\Lambda^{R_0}$ means that an increase (decrease) in Λ by a given percentage will result in an increase (decrease) of R_0 by the same percentage. Concretely, an increase of the values Λ, β_1, β_2 will increase the basic reproduction number by 100%, 15.23%, and 84.77%, respectively, and an increase of the values μ, η, δ, α, d will decrease R_0 by 6.3%, 2.53%, 6.4%, 22.52%, and 94.01%, respectively (see Table 2).

7. Simulations

In this section, we include a numerical analysis of model (4). The parameters are estimated. We will study the impact of certain parameters (α, μ, η and ε) on the solutions and the impact β of the fractional derivation order.

For this reason, we take some hypothetical data in order to illustrate the results that we have already established in the previous sections.

$$\begin{aligned}
\Lambda &= 10^5,\\
\beta_1 &= 3.8 \times 10^{-6},\\
\beta_2 &= 7 \times 10^{-6},\\
\alpha &= 0.2657,\\
\delta &= 0.3352,\\
\mu &= 0.33029,\\
\eta &= 0.13266,\\
\varepsilon &= 0.1259,\\
k &= 1.1975 \times 10^{-5},\\
r &= 0.0149,\\
d &= 3.051 \times 10^{-5},\\
(S(0), E(0), I(0), Q(0), H(0), R(0)) &= \left(11 \times 10^4, 0, 10^2, 10^2, 0, 0\right).
\end{aligned} \tag{24}$$

To resolve our fractional system (4), we have used the function "fde12" in MATLAB. It is an implementation of Adams–Bashforth–Moulton prediction correction described

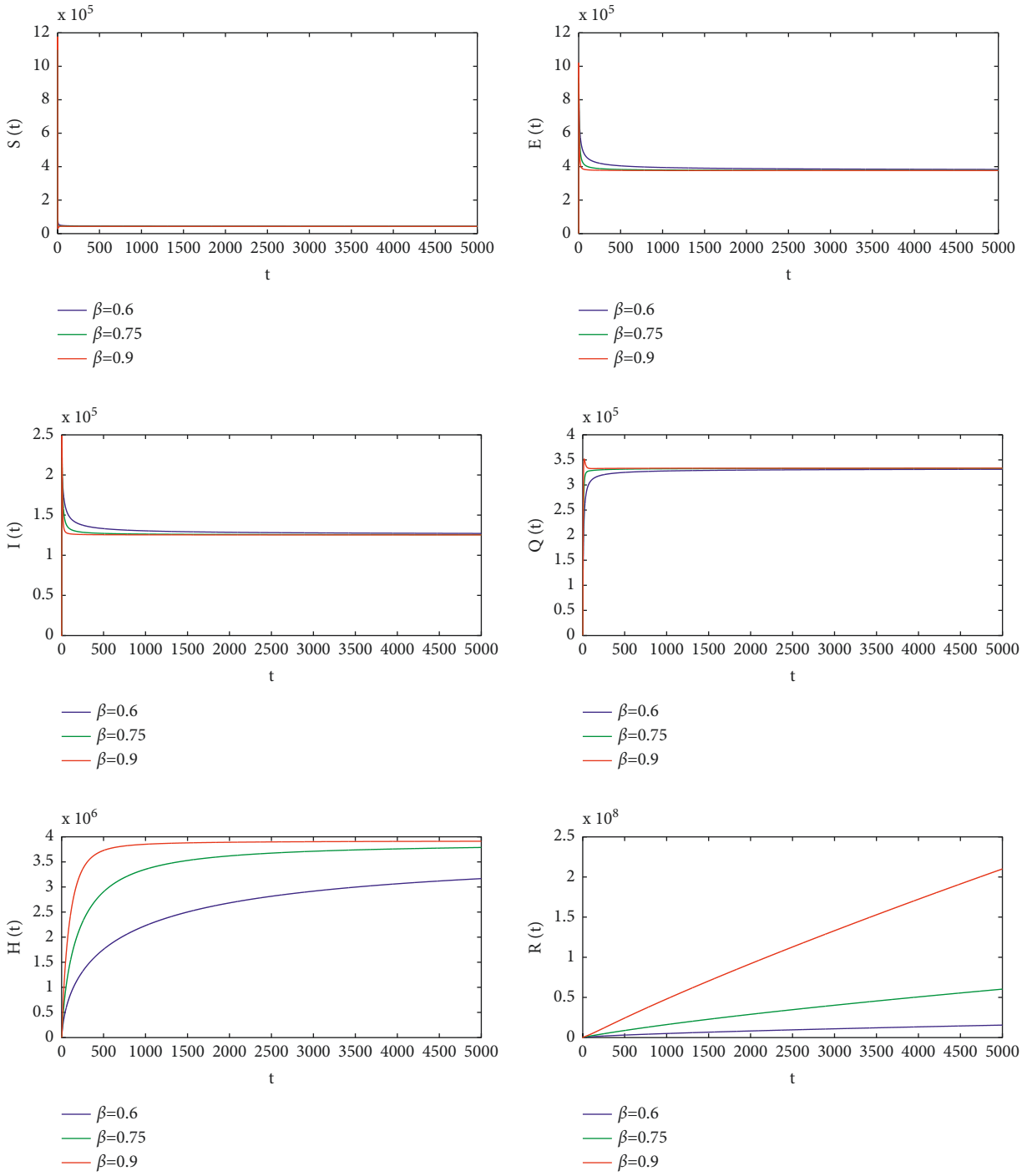

Figure 2: Impact of β according to time of endemic equilibrium P^*.

in [40]. The convergence and accuracy of this method are studied in [41]. The implementation of several iterations of the corrector has been proposed in [42]. In this implementation, the discrete convolution is evaluated using the FFT algorithm described in [43], which makes the computational cost proportional to $N * \log(N)^2$ instead of N^2 in the classical implementation; N is the number of points in time for evaluating the solution.

Figure 2 shows the impact of order fractional derivative β as a function of time t. We remark in Figure 2 that the increase of β leads to the growth of the speed of convergence for E and I. Also, we observe that the increase of β leads to a decrease in the speed of convergence for Q and H.

Figure 3 illustrates the impact of incubation rate α according to time t. We observe that the number of susceptible, exposed, and infected individuals will initially

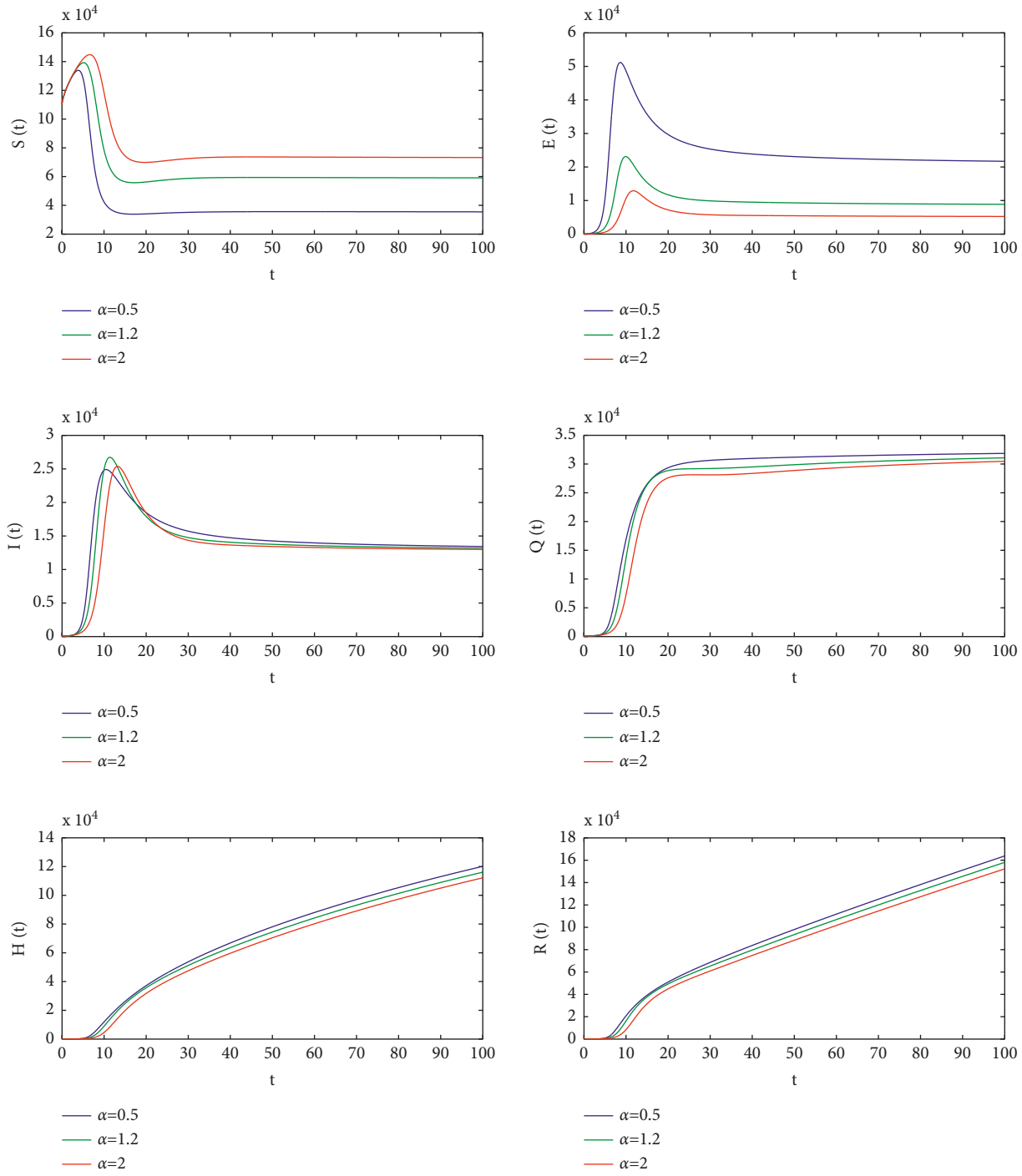

Figure 3: Impact of α according to time of endemic equilibrium P^*.

increase, but after a period of time it will decrease. We notice that the number of susceptible cases S and recovered cases R increases when α increases. Contrarily, the cases infected I, quarantined Q, hospitalized H, and exposed E are decreased. Indeed, by increasing the rate of incubation, the number of exposed cases decreases, which reduces the number of susceptible cases who will pass into the category exposed and then will be infected. This leads to a decrease in the number of infected and hospitalized cases. As a consequence, the number of recovered cases increases.

In addition, Figure 4 shows that when the value of μ increases, the number of suspected S and recovered R cases increases. Contrarily, the infected cases I, quarantined cases Q, and hospitalized cases H are decreased. This explains why if the rate μ increases, many of the infected cases will recover, causing the number of

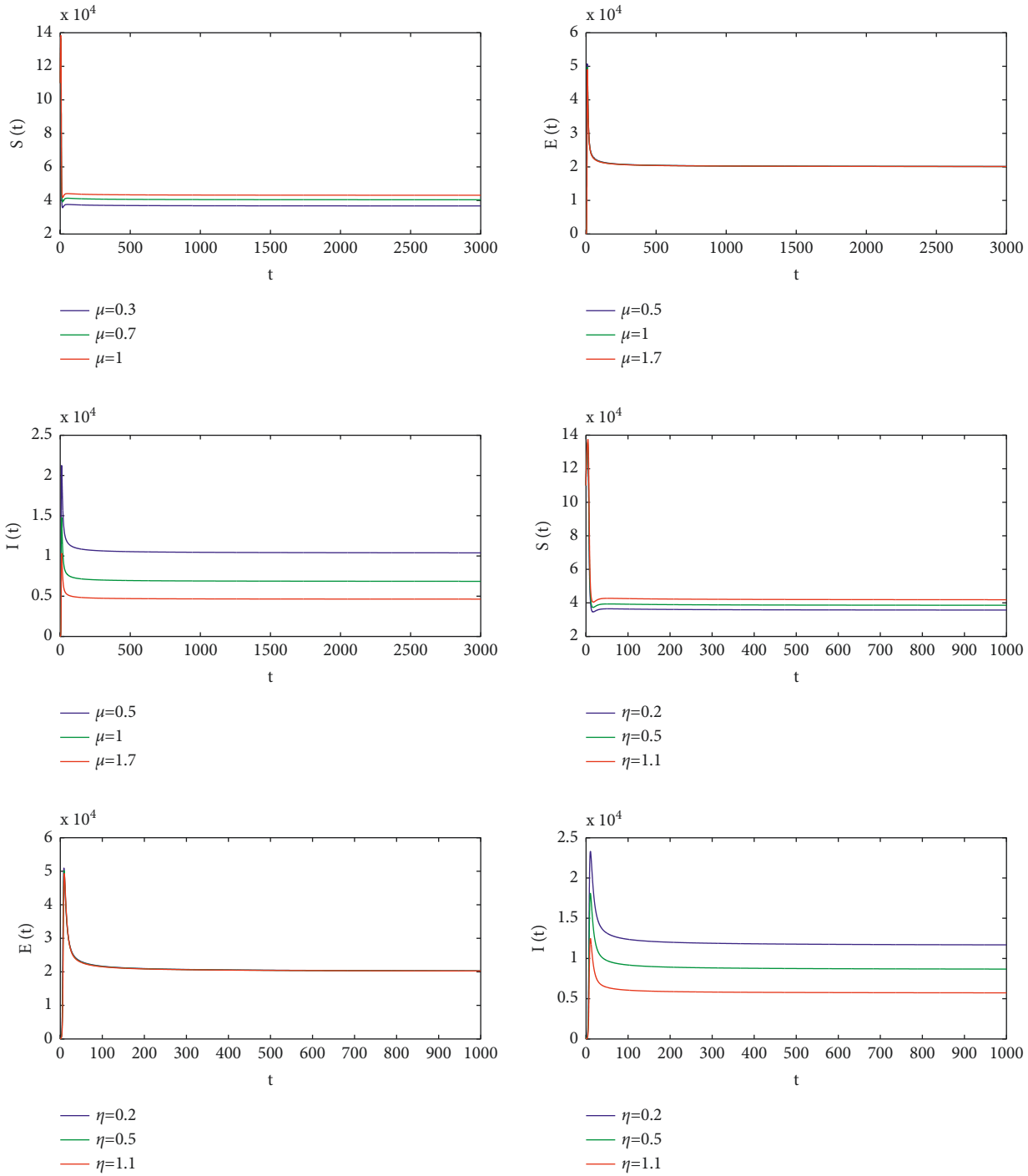

Figure 4: Impact of μ according to time of endemic equilibrium P^*.

infected individuals to decrease and the recovered cases to increase. Therefore, the number of hospitalized cases will decrease.

We can observe in Figure 5 that when the value of η increases, the number of quarantined Q and hospitalized H cases increases. On the other hand, the infected cases I and recovered cases R decrease. This implies that if the percentage of infected individuals becomes severe, they must be hospitalized. As the number of hospitalized cases grows, the number of infected cases decreases. As a result, the number of recovered cases is reduced. Moreover, in Figure 6, when the value of ε increases, the number of quarantined cases Q increases. On the other hand, the hospitalized cases H and recovered cases R decrease.

Figure 7 illustrates the impact of δ according to time t. We notice that the number of susceptible cases S,

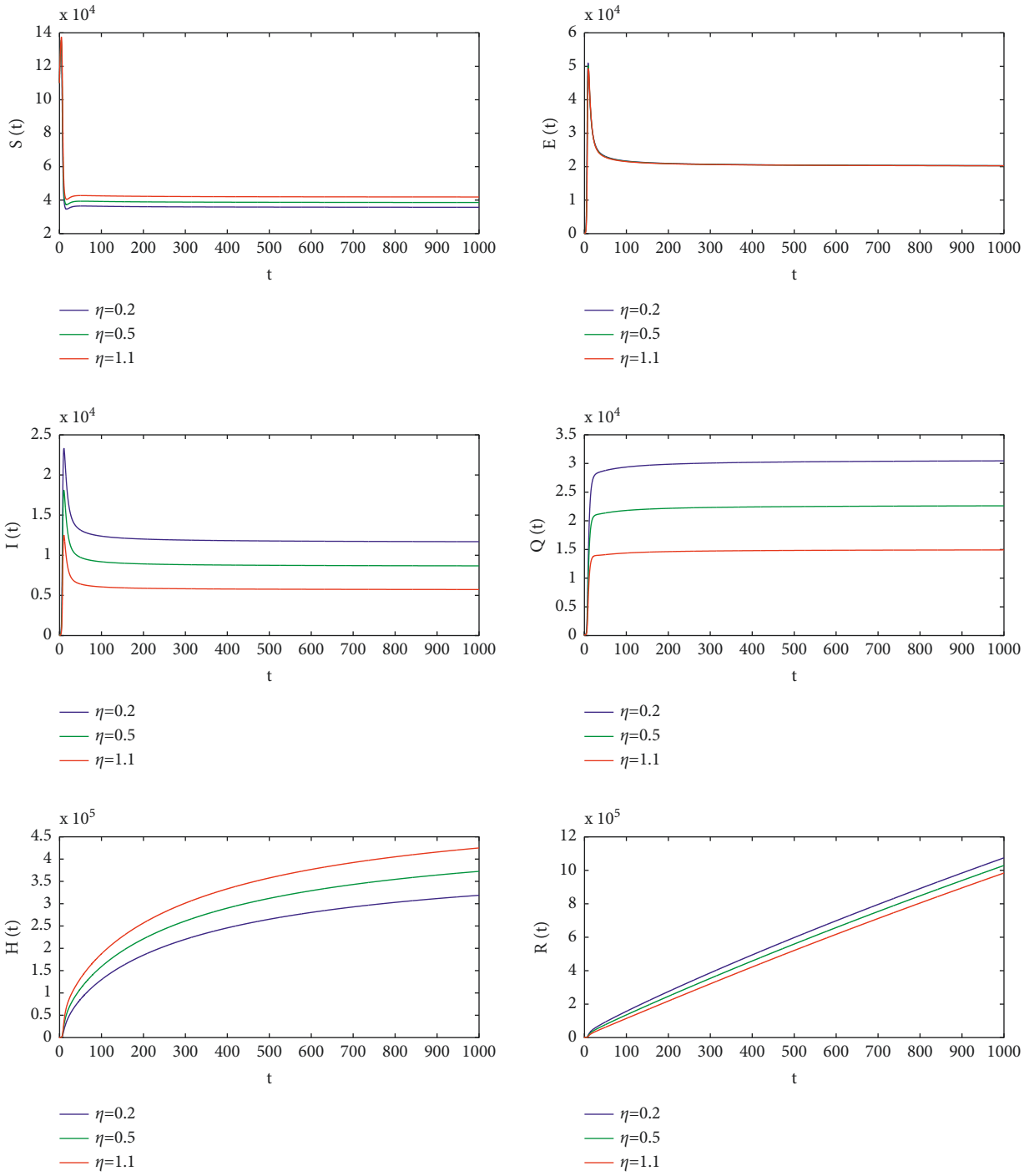

Figure 5: Impact of H according to time of endemic equilibrium P^*.

quarantined cases Q, and hospitalized cases H increases when δ increases. Contrarily, the cases infected I and recovered R are decreased, but it has little impact on the cases exposed E. This is explained by the fact that a significant number of infected (noncritical cases) must be quarantined. Among these confined cases, some individuals may be hospitalized at a constant ϵ rate. Consequently, the number of hospitalized cases is increasing.

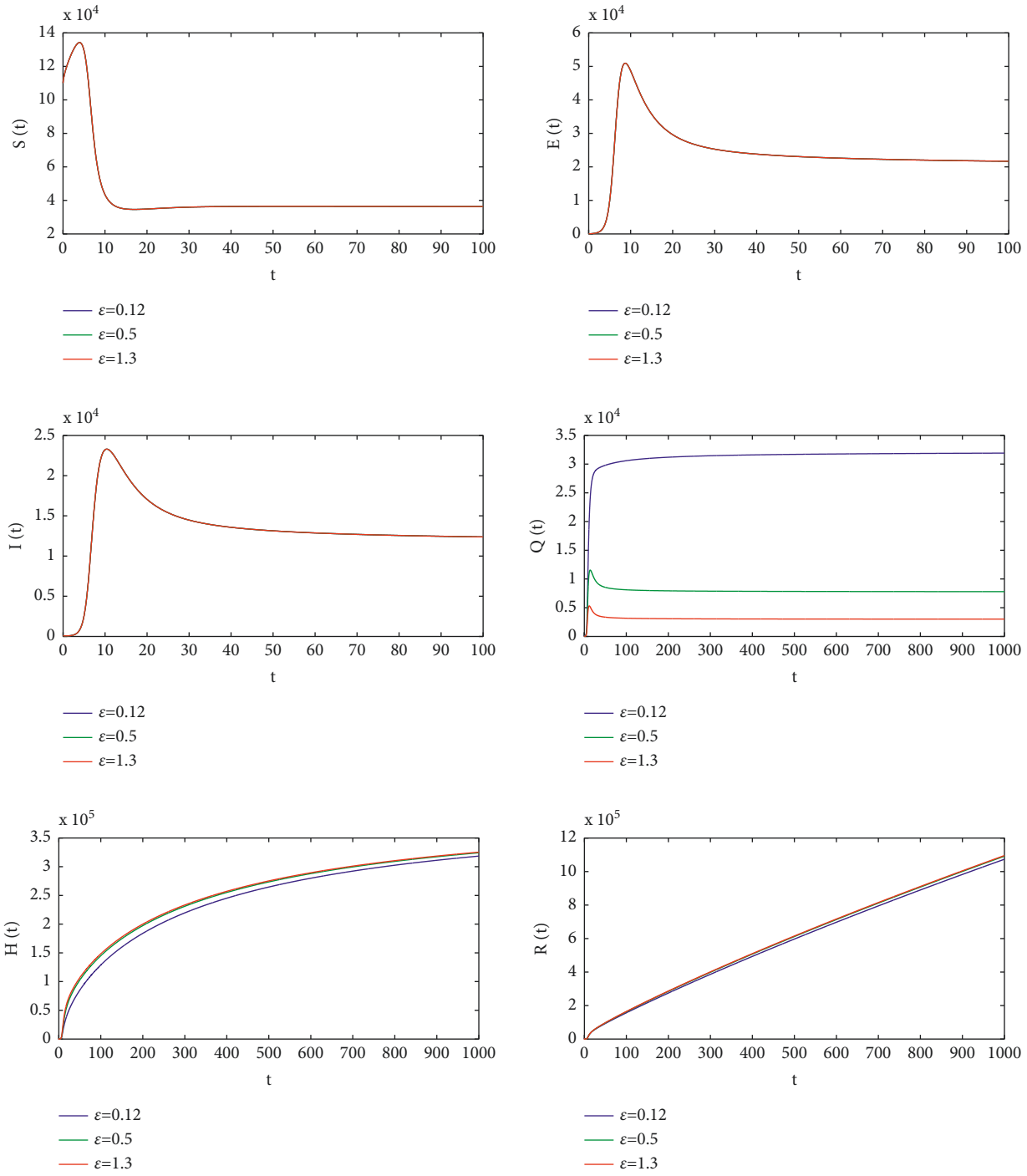

Figure 6: Impact of ε according to time of endemic equilibrium P^*.

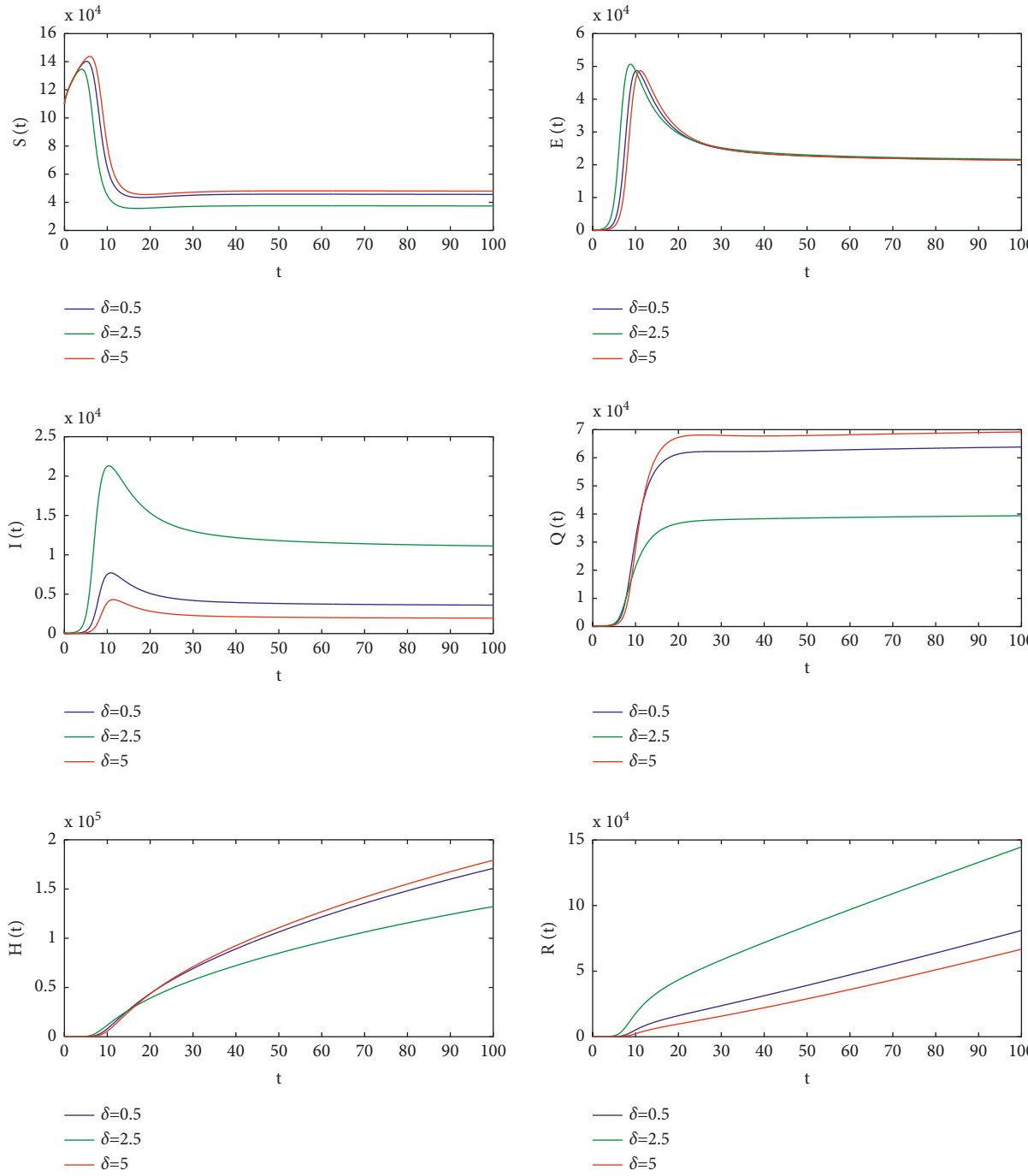

Figure 7: Impact of δ according to time of endemic equilibrium P^*.

8. Conclusion

In this paper, we have modeled the COVID-19 epidemic according to susceptible, exposed, infected, quarantined, hospitalized, and recovered compartments. An operator Caputo of fractional derivatives was used to evaluate the memory effect on the epidemic behavior. We developed a mathematical approach to prove the boundedness, uniqueness, and the existence of solutions and to demonstrate a local stability of equilibrium points.

Sensibility analysis revealed that the epidemic evolution is affected by the different model parameters. Furthermore, a numerical simulation illustrates the effect of memory in a fractional derivative, and the increase of the fractional derivation order speeds up the decrease of E, I and increase of Q, H, and R. Consequently, the calibration of this parameter provides a correct adjustment of the real data. On the other hand, they show that the susceptible cases increase with an increase in the incubation rate α, and when the rates μ and η increase, the number of infections and the exposed

cases considerably decreases. Consequently, these results can help to reduce the spread of the virus and to control the epidemic. In future work, the role of the vaccination on the expansion of this disease can be incorporated into the model. Thus, we will study a fractional model using the new definition of the fractional derivative with a non-singular kernel in the sense of Caputo [27].

Data Availability

The data used to support the findings of this study are available from Younes Louartassi upon request.

Conflicts of Interest

The authors declare that they have no conflicts of interest.

Acknowledgments

This study was funded by the Deanship of Scientific Research at Jouf University under grant no. DSR-2021-03-03124.

References

[1] C. Huang, Y. Wang, X. Li et al., "Clinical features of patients infected with 2019 novel coronavirus in wuhan, China," *The Lancet*, vol. 395, no. 10223, pp. 497–506, 2020.

[2] J. Bedford, D. Enria, J. Giesecke et al., "Covid-19: towards controlling of a pandemic," *The Lancet*, vol. 395, no. 10229, pp. 1015–1018, 2020.

[3] Y. R. Guo, Q. D. Cao, Z. S. Hong et al., "The origin, transmission and clinical therapies on coronavirus disease 2019 (COVID-19) outbreak - an update on the status," *Military Medical Research*, vol. 7, no. 1, p. 11, 2020.

[4] J. Liu, X. Liao, S. Qian et al., *Community Transmission of Severe Acute Respiratory Syndrome Coronavirus 2*, Shenzhen, china, 2020.

[5] S. Palwinder, S. Srivastava, and U. Arora, "Stability of SEIR model of infectious diseases with human immunity," *Global Journal of Pure and Applied Mathematics*, vol. 13, pp. 1811–1819, 2017.

[6] M. Ramli, S. C. Zulfa, N. A. Chaniago, and V. Halfiani, "Mathematical analysis on SEIR-type model of the Tuberculosis disease spread with vaccination and treatment elements," *Journal of Physics: Conference Series*, vol. 1235, 2019.

[7] M. Senthamarai and R. Senthamarai, "Mathematical model of epidemics: SEIR model by using homotopy perturbation method," *AIP Conference Proceedings*, vol. 2112, 2019.

[8] S. Mwalili, M. Kimathi, V. Ojiambo, D. Gathungu, and R. Waema Mbogo, "SEIR model for COVID-19 dynamics incorporating the environment and social distancing," *Interventions*, vol. 9, p. 10, 2020.

[9] J. Singh, "Analysis of fractional blood alcohol model with composite fractional derivative," *Chaos, Solitons & Fractals*, vol. 140, Article ID 110127, 2020.

[10] S. Kumar, R. P. Chauhan, J. Kumar, and D. Kumar, "A computational study of transmission dynamics for dengue fever with a fractional approach," *Mathematical Modelling of Natural Phenomena*, vol. 16, p. 48, 2021.

[11] A. Bahloul, A. Mohamed, A. Chahid, and T. M. Laleg-Kirati, "Fractional-order SEIQRDP Model for Simulating the Dynamics of COVID-19 Epidemic," 2020, https://arxiv.org/abs/2005.01820, Article ID 01820.

[12] S. H. A. Khoshnaw, R. H. Sulaimany, and S. Sulaimany, "Mathematical modelling for coronavirus disease (COVID-19) in predicting future behaviours and sensitivity analysis," *Mathematical Modelling of Natural Phenomena*, vol. 15, p. 33, 2020.

[13] Z. Lu, Y. Yu, Y. Q. Chen et al., "A fractional-order SEIHDR model for COVID-19 with inter-city networked coupling effects," *Nonlinear Dynamics*, vol. 101, no. 3, pp. 1717–1730, 2020.

[14] A. S. Shaikh, I. N. Nisar, and K. S. Nisar, "A mathematical model of COVID-19 using fractional derivative: outbreak in India with dynamics of transmission and control," *Advances in Difference Equations*, vol. 2020, no. 1, p. 373, 2020.

[15] C. Xu, Y. Yu, Y. Lu, and Z. Lu, "Forecast analysis of the epidemics trend of COVID-19 in the USA by a generalized fractional-order SEIR model," *Nonlinear Dynamics*, vol. 101, no. 3, pp. 1621–1634, 2020.

[16] G. González-Parra, A. J. Chen-Charpentier, and B. M. Chen-Charpentier, "A fractional order epidemic model for the simulation of outbreaks of influenza A (H1N1)," *Mathematical Methods in the Applied Sciences*, vol. 37, no. 15, pp. 2218–2226, 2014.

[17] R. L. Magin, *Fractional calculus in bioengineering*, Vol. 2, Begell House Redding, Danbury, Connecticut, 2006.

[18] K. Oldham and J. Spanier, "The fractional calculus theory and applications of differentiation and integration to arbitrary order," *Elseiver*, vol. 111, 1974.

[19] M. Riesz, "L'intégrale de Riemann-Liouville et le problème de Cauchy," *Acta Mathematica*, vol. 81, no. 0, pp. 1–222, 1949.

[20] B. Ross, S. G. Love, and E. R. Love, "Functions that have no first order derivative might have fractional derivatives of all orders less than one," *Real Analysis Exchange*, vol. 20, no. 1, p. 140, 1994.

[21] S. Samko, A. Kilbas, and O. Marichev, *Fractional Integrals and Derivatives : Theory and Applications*, p. 1, 1993.

[22] E. Elgazzar and A. Elgazzar, "On fractional order differential equations model for nonlocal epidemics," *Physica A: Statistical Mechanics and Its Applications*, vol. 379, no. 2, pp. 607–614, 2007.

[23] N. D. Cong, T. S. Doan, S. Tuan, and H. T. Tuan, "Linearized asymptotic stability for fractional differential equations," *Electronic Journal of Qualitative Theory of Differential Equations*, vol. 39, no. 39, pp. 1–13, 2016.

[24] R. Khalil, M. Al Horani, A. Yousef, and M. Sababheh, "A new definition of fractional derivative," *Journal of Computational and Applied Mathematics*, vol. 264, pp. 65–70, 2014.

[25] T. Abdeljawad, "On conformable fractional calculus," *Journal of Computational and Applied Mathematics*, vol. 279, pp. 57–66, 2015.

[26] A. Ben Makhlouf, O. Naifar, M. A. Wu, and B. W. Wu, "FTS and FTB of conformable fractional order linear systems," *Mathematical Problems in Engineering*, vol. 2018, pp. 1–5, 2018.

[27] K. Hattaf, "On some properties of the new generalized fractional derivative with non-singular kernel," *Mathematical Problems in Engineering*, vol. 2021, pp. 1–6, 2021.

[28] K. Hattaf, "Stability of fractional differential equations with new generalized hattaf fractional derivative," *Mathematical Problems in Engineering*, vol. 2021, pp. 1–7, 2021.

[29] K. Hattaf, "On the stability and numerical scheme of fractional differential equations with application to biology," *Computation*, vol. 10, no. 6, p. 97, 2022.

[30] J. J. Wang, J. Z. Jin, and Z. Jin, "Analysis of an SIR model with bilinear incidence rate," *Nonlinear Analysis: Real World Applications*, vol. 11, no. 4, pp. 2390–2402, 2010.

[31] I. Podlubny, *Fractional Differential Equations: An Introduction to Fractional Derivatives, Fractional Differential Equations, to methods of their Solution and Some of their application*, vol. 198, Elsevier, Amsterdam, Netherlands, 1998.

[32] Y. Li, Y. Podlubny, and I. Podlubny, "Stability of fractional-order nonlinear dynamic systems: lyapunov direct method and generalized Mittag-Leffler stability," *Computers & Mathematics with Applications*, vol. 59, no. 5, pp. 1810–1821, 2010.

[33] E. Ahmed, A. El-Sayed, and H. A. El-Saka, "Equilibrium points, stability and numerical solutions of fractional-order predator-prey and rabies models," *Journal of Mathematical Analysis and Applications*, vol. 325, no. 1, pp. 542–553, 2007.

[34] D. Matignon, "Stability results for fractional differential equations with applications to control processing," *Proceedings of the Computational Engineering in Systems and Application Multiconference*, vol. 2, pp. 963–968, 1996.

[35] M. A. Khan, Q. Badshah, S. Islam, I. Khan, S. Shafie, and S. A. Khan, "Global dynamics of SEIRS epidemic model with non-linear generalized incidences and preventive vaccination," *Advances in Difference Equations*, vol. 2015, no. 1, p. 88, 2015.

[36] M. A. Khan, Y. Islam, and S. Islam, "Complex dynamics of an SEIR epidemic model with saturated incidence rate and treatment," *Physica A: Statistical Mechanics and Its Applications*, vol. 493, pp. 210–227, 2018.

[37] X. Yang and L. Yang, "Stability analysis of an SEIQV epidemic model with saturated incidence rate," *Nonlinear Analysis: Real World Applications*, vol. 13, no. 6, pp. 2671–2679, 2012.

[38] E. Ahmed, A. El-Sayed, and H. AA. El-Saka, "On some Routh-Hurwitz conditions for fractional order differential equations and their applications in Lorenz, Rössler, Chua and Chen systems," *Physics Letters A*, vol. 358, no. 1, pp. 1–4, 2006.

[39] S. Makinde and O. D. Makinde, "A mathematical model for coinfection of listeriosis and anthrax diseases," *International Journal of Mathematics and Mathematical Sciences*, vol. 2018, pp. 1–14, 2018.

[40] K. Diethelm and A. D. Freed, "The Frac PECE subroutine for the numerical solution of differential equations of fractional order," in *Forschung und Wissenschaftliches Rechnen 1998*, S. Heinzel and T. Plesser, Eds., pp. 57–71, Gessellschaft fur Wissenschaftliche Datenverarbeitung, Gottingen, 1999.

[41] K. Diethelm, N. J. Ford, and A. D. Freed, "Detailed error analysis for a fractional Adams method," *Numerical Algorithms*, vol. 36, no. 1, pp. 31–52, 2004.

[42] K. Diethelm, "Efficient solution of multi-term fractional differential equations using P (EC) m E methods," *Computing*, vol. 71, no. 4, pp. 305–319, 2003.

[43] E. Hairer, C. Lubich, and M. Schlichte, "Fast numerical solution of nonlinear Volterra convolution equations," *SIAM Journal on Scientific and Statistical Computing*, vol. 6, no. 3, pp. 532–541, 1985.